

PyCosmo: An Integrated Cosmological Boltzmann Solver

Alexandre Refregier¹, Lukas Gamper¹, Adam Amara¹, Lavinia Heisenberg²

¹*Department of Physics, ETH Zurich, Wolfgang Pauli Strasse 27, 8093 Zurich, Switzerland*

²*Institute for Theoretical Studies, ETH Zurich, Clausiusstrasse 47, 8092 Zurich, Switzerland*

Abstract

As wide-field surveys yield ever more precise measurements, cosmology has entered a phase of high precision requiring highly accurate and fast theoretical predictions. At the heart of most cosmological model predictions is a numerical solution of the Einstein-Boltzmann equations governing the evolution of linear perturbations in the Universe. We present PyCosmo, a new Python-based framework to solve this set of equations using a special purpose solver based on symbolic manipulations, automatic generation of C++ code and sparsity optimisation. The code uses a consistency relation of the field equations to adapt the time step and does not rely on physical approximations for speed-up. After reviewing the system of first-order linear homogeneous differential equations to be solved, we describe the numerical scheme implemented in PyCosmo. We then compare the predictions and performance of the code for the computation of the transfer functions of cosmological perturbations and compare it to existing cosmological Boltzmann codes. We find that we achieve comparable execution times for comparable accuracies. While PyCosmo does not yet have all the features of other codes, our approach is complementary to existing cosmological Boltzmann solvers and can be used as an independent test of their numerical solutions. The symbolic representation of the Einstein-Boltzmann equation system in PyCosmo provides a convenient interface for implementing extended cosmological models. We also discuss how the PyCosmo framework can also be used as a general framework to compute cosmological quantities as well as observables for both interactive and high-performance batch jobs applications. Information about the PyCosmo package and future code releases are available at <http://www.cosmology.ethz.ch/research/software-lab.html>.

Keywords: Cosmology, Boltzmann Equation, Differential Equations, Python

1. Introduction

In order to address the fundamental questions raised by the nature of Dark Matter, Dark Energy and large scale gravity, a number of cosmological experiments are currently underway or in the planning (eg. DES¹, DESI², LSST³, Euclid⁴, WFIRST⁵). These experiments aim to achieve the high precision required to tackle these questions and will thus require highly accurate predictions of observables for a wide set of cosmological models. At the heart of most cosmological model prediction is a numerical solution of the Einstein-Boltzmann equations (see [1] and reference therein) governing the linear evolution of perturbations in the Universe. Several codes have thus been developed to produce fast and accurate solutions to this set of first-order linear homogeneous differential equations, such as COSMICS [2], CMBFAST [3], CMBEASY [4], CAMB [5], CLASS [6], with only the latter two being currently maintained. The predictions of these codes are then compared to measurements from cosmological surveys to derive constraints on the parameters of the cosmological model using Monte-Carlo Markov Chain techniques (eg. [7, 8]). Given the central importance of Boltzmann codes to our current constraints on the cosmological model and the well known numerical

¹<http://www.darkenergysurvey.org>

²<http://desi.lbl.gov>

³<http://www.lsst.org>

⁴<http://sci.esa.int/euclid/>

⁵<http://wfirst.gsfc.nasa.gov>

difficulty to solve this set of equations (see e.g. [9] for a mathematical analysis, and references therein), it is important to explore different numerical schemes for the solutions of the differential equations.

In this paper, we present **PyCosmo**, a new Python-based framework to solve the Einstein-Boltzmann equations using a special purpose solver based on symbolic manipulations, automatic generation of C++ code and sparsity optimisation. The code uses a consistency relation of the field equations to adapt the time step and does not rely on physical approximations for speed-up. We study the accuracy and performance of **PyCosmo** for the computation of the transfer functions of cosmological perturbations in the newtonian gauge in a flat universe, and compare it to existing codes. Our approach is complementary to existing cosmological Boltzmann solvers that are based on more general differential equation solvers and physical approximations, and can be used as an independent test of their numerical solutions. We discuss how the symbolic representation of the Einstein-Boltzmann equation system in **PyCosmo** provides a convenient interface for theorists to rapidly implement new cosmological models. We also discuss how the **PyCosmo** framework can also be used as a general framework to compute cosmological quantities as well as observables for both interactive and for high-performance batch jobs applications, drawing upon the earlier IDL cosmological package **ICosmo** [10].

The paper is organised as follows. In section 2, we describe the set of Einstein-Boltzmann equations describing the linear growth of cosmological structures. Section 3 describes our implementation scheme for deriving numerical solutions to this set of equations. In section 4 we study the performance of **PyCosmo** in terms of numerical precision and speed and compare it to existing codes. Our conclusions are described in section 5.

2. Einstein-Boltzmann Equations

2.1. Linear Perturbations

After solving the evolution of the scale factor a and the Hubble parameter H using the Friedmann equation (see eg. [11]), we can consider the linear evolution of scalar perturbations. For this purpose, we choose the newtonian gauge in a flat Λ CDM cosmology. The evolution of perturbations are thus governed by the Einstein-Boltzmann equations which, in this case and to linear order, are given by ([1] with the conventions of [11])

$$\dot{\delta} = -ku - 3\dot{\Phi} \quad (1)$$

$$\dot{u} = -\frac{\dot{a}}{a}u + k\Psi \quad (2)$$

$$\dot{\delta}_b = -ku_b - 3\dot{\Phi} \quad (3)$$

$$\dot{u}_b = -\frac{\dot{a}}{a}u_b + k\Psi + kc_s^2\delta_b + \frac{\dot{\tau}}{R}[u_b - 3\Theta_1] \quad (4)$$

$$\dot{\Theta}_0 = -k\Theta_1 - \dot{\Phi} \quad (5)$$

$$\dot{\Theta}_1 = \frac{k}{3}[\Theta_0 - 2\Theta_2 + \Psi] + \dot{\tau}\left[\Theta_1 - \frac{u_b}{3}\right] \quad (6)$$

$$\dot{\Theta}_2 = \frac{k}{5}[2\Theta_1 - 3\Theta_3] + \dot{\tau}\left[\Theta_2 - \frac{\Pi}{10}\right] \quad (7)$$

$$\dot{\Theta}_l = \frac{k}{2l+1}[l\Theta_{l-1} - (l+1)\Theta_{l+1}] + \dot{\tau}\Theta_l, \quad l > 2 \quad (8)$$

$$\dot{\Theta}_{Pl} = \frac{k}{2l+1}[l\Theta_{P(l-1)} - (l+1)\Theta_{P(l+1)}] + \dot{\tau}\left[\Theta_{Pl} - \frac{\Pi}{2}(\delta_{l,0} + \frac{\delta_{l,2}}{5})\right] \quad (9)$$

$$\dot{\mathcal{N}}_0 = -k\mathcal{N}_1 - \dot{\Phi} \quad (10)$$

$$\dot{\mathcal{N}}_1 = \frac{k}{3}[\mathcal{N}_0 - 2\mathcal{N}_2 + \Psi] \quad (11)$$

$$\dot{\mathcal{N}}_l = \frac{k}{2l+1}[l\mathcal{N}_{l-1} - (l+1)\mathcal{N}_{l+1}], \quad l > 1 \quad (12)$$

$$k^2\Phi + 3\frac{\dot{a}}{a}\left(\Phi - \frac{\dot{a}}{a}\Psi\right) = 4\pi Ga^2[\rho_m\delta_m + 4\rho_r\Theta_{r0}], \quad (13)$$

where dot denotes derivatives with respect to conformal time η , δ (δ_b) and u (u_b) are the density and velocity perturbations for the dark matter (baryons), Θ_l and Θ_{Pl} are the photon temperature and polarization multipole moments, \mathcal{N}_l are the multipole moments of the (massless) neutrino temperature, and $\Pi = \Theta_2 + \Theta_{P0} + \Theta_{P2}$. The baryon-to-photon ratio is given by $R = 3\rho_b/(4\rho_\gamma)$, τ is the Thomson scattering optical depth and c_s is the baryon sound speed. The subscripts r and m refer to the density-weighted sum of all radiation and matter components, and ρ_r and ρ_m is the mean density in each of these components.

The gravitational potential fields Φ and Ψ describe scalar perturbations to the metric $ds^2 = -(1 + 2\Psi)dt^2 + a^2(1 + 2\Phi)d\vec{x}^2$, and are related by the longitudinal traceless space-space parts of the Einstein equation by means of the algebraic equation

$$k^2(\Phi + \Psi) = -32\pi G a^2 \rho_r \Theta_{r2}. \quad (14)$$

Note that an alternative to the time-time Einstein equation (Eq. 13) is its time-space component given by

$$\dot{\Phi} - \frac{\dot{a}}{a}\Psi = -4\pi G \frac{a^2}{k} [\rho_m u_m + 4\rho_r \Theta_{r1}]. \quad (15)$$

2.2. Initial Conditions

We assume initial conditions arising from inflation for which the primordial power spectrum of the potential Φ follows

$$P_\Phi(k) = \frac{50\pi^2}{9k^3} \left(\frac{k}{H_0} \right)^{n-1} \delta_H^2 \left(\frac{\Omega_m}{D(a=1)} \right)^2, \quad (16)$$

where δ_H is a normalisation parameter, $D(a)$ is the late time growth factor (normalised to $D(a) = a$ in the matter era), n is the scalar spectral index, and H_0 is the present value of the Hubble parameter. For adiabatic initial conditions, the other fields at early times are given by [1]

$$\begin{aligned} \Phi &= -\left(1 + \frac{2}{5}R_\nu\right)\Psi \\ \delta &= \delta_b = 3\Theta_0 = 3\mathcal{N}_0 = -\frac{3}{2}\Psi \\ u &= u_b = 3\Theta_1 = 3\mathcal{N}_1 = \frac{1}{2}k\eta\Psi \\ \mathcal{N}_2 &= \frac{1}{30}k\eta\Psi, \end{aligned} \quad (17)$$

where $R_\nu = (\rho_\nu + P_\nu)/(\rho + P) = \Omega_\nu/(\frac{3}{4}\Omega_m a + \Omega_r)$ is the neutrino ratio, and all the other perturbation fields are set to 0 at the initial time.

2.3. Practicalities

In practice, the hierarchy of moments for the photons and the neutrinos can be truncated to a maximum multipole l_{\max} by replacing Equations (8-9) for $\dot{\Theta}_l$ at $l = l_{\max}$ with [1]

$$\dot{\Theta}_l \simeq k\Theta_{l-1} - \frac{l+1}{\eta}\Theta_l + \tau\Theta_l, \quad (18)$$

and similarly for Θ_{Pl} and for \mathcal{N}_l , but without the Thomson scattering term in the latter case.

The optical depth τ and the sound speed c_s can be pre-computed using public recombination codes such as RECFAST [12, 13], RECFAST++ [12, 14, 15, 16, 17] or COSMOSPEC [18]. In PyCosmo, we have implemented an interface to RECFAST++, as well as the possibility of external input recombination variables for comparisons with other Boltzmann codes.

To test for numerical accuracy, we use the redundancy of the Einstein field equations following [1, 19]. From the algebraic relation in equation (14), we can express the non-dynamical gravitational field Ψ in terms of Φ . From the time-space component of the Einstein equations (Eq. 15), we can express the time derivative of the gravitational field Φ in terms of the other fields. The expression for $\dot{\Phi}$ can then be plugged back into the time-time component of the

Einstein equations (Eq. 13), which results in an algebraic equation for Φ . This reflects the fact, that the gravitational field Φ is not a dynamical degree of freedom and can be solved algebraically in terms of the remaining relativistic and non-relativistic matter fields. We will use this combination of the two Einstein equations (13) and (15) in order to test our numerical accuracy. We will denote the resulting algebraic equation by the dimensionless parameter defined as [1, 19]

$$\epsilon = \left[-\frac{2}{3} \left(\frac{k}{aH_0} \right)^2 \Phi + (\Omega_m \delta_m a^{-3} + 4\Omega_r \Theta_{r0} a^{-4}) + 3 \frac{aH}{k} (\Omega_m u_m a^{-3} + 4\Omega_r \Theta_{r1} a^{-4}) \right] (\Omega_m a^{-3} + \Omega_r a^{-4} + \Omega_\Lambda)^{-1} \quad (19)$$

which ought to vanish for the consistency of the equations and thus gives a relative measure of numerical errors. We thus use ϵ to adapt our time steps and choose to use eq. (13) in our Einstein-Boltzmann system.

The initial conditions given in equation (17) are implemented using the scheme in CLASS [6] which includes higher order terms for improved numerical precisions at early time. We also choose the initial time of the initial condition as in COSMICS, i.e. an initial conformal time $\eta = \min[10^{-3} k^{-1}, 10^{-1} h^{-1} \text{Mpc}]$.

3. Numerical solution scheme

In this section, we describe our method to solve the Einstein-Boltzmann Equations (Eqs. 1-13) to derive the transfer functions for the different perturbation fields.

3.1. Differential equation system

For each wavenumber k , we solve the linear homogeneous non-autonomous system of $8 + 3l_{\text{max}}$ coupled differential equations (Eqs. 1-13, with the algebraic equation 14) which can be recast in the form

$$\dot{\mathbf{y}}(k, \eta) = \mathbf{J}(k, \eta) \mathbf{y}(k, \eta) \quad (20)$$

where $\mathbf{y}(k, \eta) = (\Phi, \delta, u, \delta_b, u_b, \Theta_0, \Theta_{P0}, \mathcal{N}_0, \Theta_1, \Theta_{P1}, \mathcal{N}_1, \dots, \Theta_{l_{\text{max}}}, \Theta_{Pl_{\text{max}}}, \mathcal{N}_{l_{\text{max}}})$ is the vector of the $8 + 3l_{\text{max}}$ perturbation fields, dot denotes, as earlier, a derivative in terms of the conformal time η , and $\mathbf{J}(k, \eta)$ is a k - and time-dependent Jacobian matrix. This was easily achievable by solving for Φ in Equation 13 and substituting it in the equations which have an explicite dependence on it. For convenience, we perform a change of variable to change the time variable η to $\ln a$ for the purpose of the integration, which has the advantage of reducing the dynamic range of the time steps during the integration in practice.

3.2. Solver

To solve the set of Einstein-Boltzmann equations, we have implemented a novel solver scheme based on a combination of symbolic manipulations, automatic C++ code generation and numerical integration tuned to this problem.

One of the central components in this scheme is to represent the set of linear differential equations of the perturbations (Eqs. 1-13) in symbolic form. We implement this using the `sympy` package. This has the advantage of allowing the package to symbolically manipulate the equations within the `Python` framework. Moreover, starting from a symbolic representation provides a convenient interface for theorists who wish to modify the set of equations to be integrated. This also allows the code to generate symbolic equations automatically for each of the multipole moments $l > 2$ for the photons and neutrinos up to a set maximum multipole moment l_{max} using their recurrence relations. Furthermore, the jacobian matrix \mathbf{J} (Eq. 20) is generated in symbolic form by applying the `jacobian` function of `sympy` to the set of differential equations. The symbolic form is also used to change the time variable from η to $\ln a$ as discussed above.

As the numerical integration scheme we use the second order Backward-Differentiation-Formula method (BDF2) with variable time-step (see e.g. [20]). This integration scheme has the advantage of being implicit, multi-step, second order and A-stable unlike multi-step methods of higher-order. It can be written as

$$\frac{1 + 2\tau_n}{1 + \tau_n} \mathbf{y}_{n+1} - (1 + \tau_n) \mathbf{y}_n + \frac{\tau_n^2}{1 + \tau_n} \mathbf{y}_{n-1} = \Delta t_n \mathbf{J} \mathbf{y}_{n+1}, \quad (21)$$

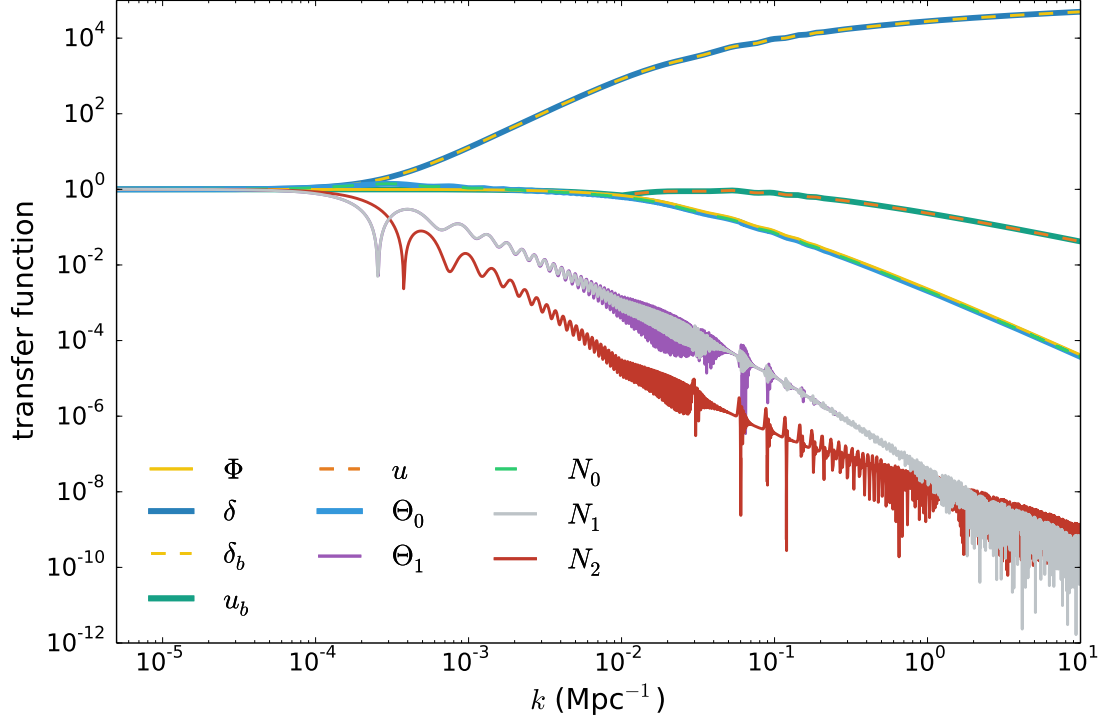


Figure 1: Transfer function $T(k)$ for the main perturbation fields at $a = 1$ as computed by PyCosmo. They were normalised such that $T(k) \rightarrow 1$ as $k \rightarrow 0$ and the reference accuracy setting for PyCosmo were used (see text).

where $\mathbf{y}_n = \mathbf{y}(t_n)$, $\Delta t_n = t_{n+1} - t_n$ is the variable time step, $\tau_n = \Delta t_n / \Delta t_{n-1}$, and the time variable is $t = \ln a$ in our implementation. We recast this equation into the form

$$\mathbf{A}\mathbf{y}_{n+1} = \mathbf{b}(\mathbf{y}_n, \mathbf{y}_{n-1}), \quad (22)$$

where $\mathbf{A} = (1 + 2\tau_n)(1 + \tau_n)^{-1}\mathbb{I} - \Delta t_n \mathbf{J}$ and $\mathbf{b} = (1 + \tau_n)\mathbf{y}_n - \tau_n^2(1 + \tau_n)^{-1}\mathbf{y}_{n-1}$. We symbolically generate the matrix \mathbf{A} and simplify it using the `simplify` function in `sympy`.

To solve this equation for \mathbf{y}_{n+1} in terms of \mathbf{y}_{n-1} and \mathbf{y}_n , we use LU factorisation with Partial Pivoting followed by a triangle-solve algorithm (see e.g. [21] for a description). We first do this symbolically assuming that no partial pivoting is necessary in the LU factorisation. In particular, we evaluate the \mathbf{A} matrix by isolating common sub-expressions using the `cse` function in `sympy`.

Another central feature of our method is to automatically generate optimised C++ code, an approach that uses heritage from our just-in-time Python compiler HOPE [22]. This is done by transforming the symbolic `sympy` expressions into C++ code using a visitor pattern. In the process, the C++ is optimised by replacing integer powers by multiple products. The C++ code is then generated to perform the LU factorisation considering only the non-zero elements in the \mathbf{A} matrix and by unrolling the loops. This improves performance significantly as the \mathbf{A} matrix has $(8 + 3l_{\max})^2$ elements but is very sparse with only of order $8l_{\max}$ non-zero elements (see recurrence relations for the photons and neutrino moments) (Eqs. 8 & 12). We then generate the solution for \mathbf{y}_{n+1} using the triangle-solve algorithm. We use the Python `distutils` package to compile the C++ code into a dynamic library which we import into Python.

During runtime, the algorithm checks whether partial pivoting is necessary. If this is the case, it builds a graph to track the additional row permutations that are needed. New C++ code can then be generated for each new permutation

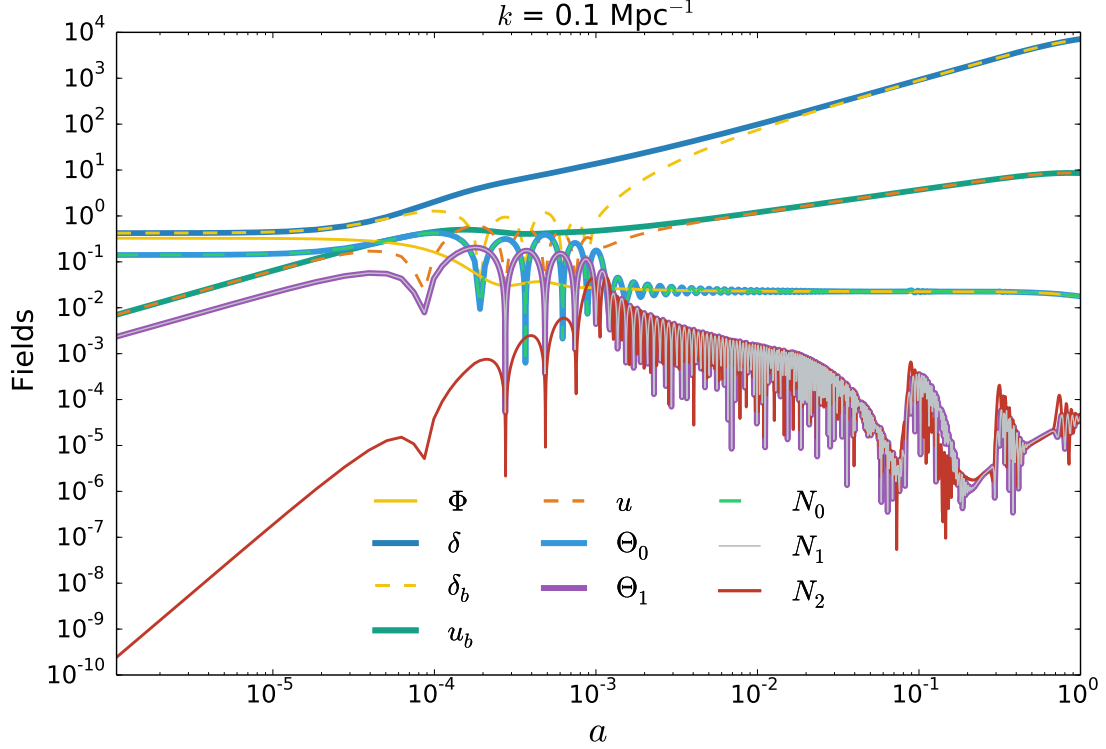


Figure 2: Main perturbation fields as a function of the scale factor a computed by PyCosmo with the reference accuracy setting and for the wavenumber $k = 0.1 \text{ Mpc}^{-1}$.

optimised as described above. For speed up, we implemented a caching scheme for the symbolic BDF equations. In practice, only a few dozen permutations are needed.

For the adaptive control of the time step Δt , we impose the following constraints:

- The parameter ϵ (Eq. 19) that we derived from the consistency of the field equations is used as a dimensionless measure of numerical errors. We impose that it remains within a set upper and lower limit after smoothing on a set time scale Δt_{smooth} typically set to 0.1. If the upper limit is exceeded, we step back by Δt_{smooth} and reduce the timestep Δt by 50% at that point. If ϵ becomes smaller than the lower limit, we increase the timestep by 25%. For safety, we do not allow the time step to be further modified for another smoothing time scale.
- We also impose that the time step Δt is smaller than the expansion time $\eta a H$ and the Courant time aH/k (for $t = \ln a$) as in COSMICS. If these limits are exceed we reduce the time scale by 50% using the smoothing time scale described above.

4. Results

After presenting the implementation of our solver, we now summarise our results on its performance for the transfer functions $T(k)$ of the perturbations. Figure 1 shows the transfer functions as function of the wavenumber k for the main perturbation fields at $a = 1$ as computed by PyCosmo. For this purpose and below, we assumed a flat Λ CDM cosmology with $\Omega_m = 0.3$, $\Omega_\Lambda = 0.7$, $\Omega_b = 0.06$ and $h = 0.7$. The transfer functions were normalised such that $T(k) \rightarrow 1$ as $k \rightarrow 0$. For this figure, we have used a high accuracy PyCosmo setting of $l_{\text{max}} = 200$ and $\epsilon < 10^{-6}$ which we use as a reference setting.

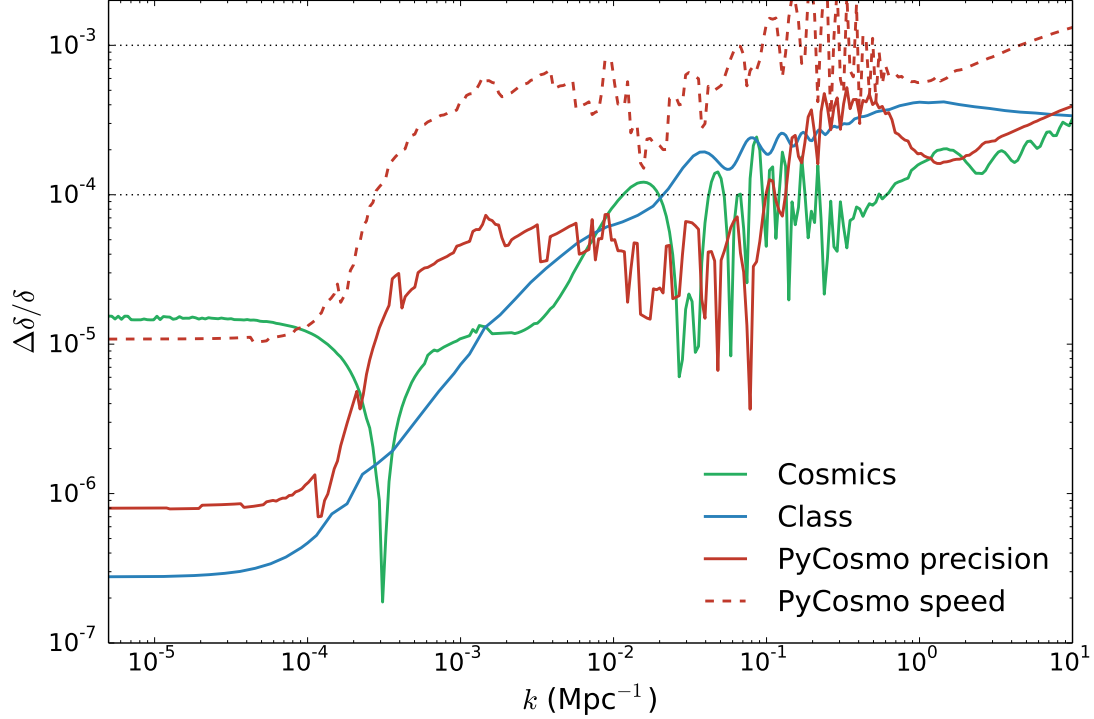


Figure 3: Relative difference dark matter density δ at $a = 1$ between the different Boltzmann codes. For PyCosmo different accuracy settings are shown (see text).

Figure 2 illustrates the time evolution of the perturbations by showing the main perturbation fields as a function of the scale factor a computed by PyCosmo with the same setting. The normalisation was chosen to match that of Φ in the earlier figure and the wave number was chosen to be $k = 0.1 \text{ Mpc}^{-1}$.

Figure 3 shows the relative difference in the dark matter density perturbation field δ in the newtonian gauge between the Boltzmann codes PyCosmo, CLASS and COSMICS, as a function of wavenumber k at $a = 1$. All results are shown relative to PyCosmo with the reference setting given above. CLASS was run using the high accuracy precision file `pk_ref.pre` available in the public distribution version 2.5.0, while COSMICS was run using its default settings. For PyCosmo, we consider a setting chosen for precision with $l_{\text{max}} = 50$ and $\epsilon < 3 \times 10^{-5}$, and a setting chosen for speed with $l_{\text{max}} = 30$ and $\epsilon < 3 \times 10^{-4}$. Also in this and the other comparisons below, the recombination variables c_s and τ for PyCosmo were taken to be that of CLASS to focus the comparison on the Boltzmann solvers rather than the recombination codes. Since CAMB does not have a newtonian gauge setting, we do not include this code in this comparison, but it was shown to agree with CLASS at the 0.01% level for the matter transfer function with this high precision setting [23].

As the figure shows, we find that CLASS, COSMICS and PyCosmo with the precision setting achieve an accuracy better than about 0.01% for $k < 10^{-2} \text{ Mpc}^{-1}$ and 0.05% for $k < 10 \text{ Mpc}^{-1}$ compared to the reference run. These differences are comparable to those found between CLASS and CAMB at high accuracy settings by [23]. When used in the speed setting, the figure shows that PyCosmo achieves an accuracy of about 0.1% for $k < 10 \text{ Mpc}^{-1}$.

The performance of the different codes can be compared by considering their execution time for different accuracy settings. For this purpose, we consider the timings derived from the best of 5 executions on a single core of a MacBook Pro with 2.7 GHz intel Core i7 and 16GB of RAM. Table 1, describes the resulting execution times for PyCosmo with

Table 1: Execution times (sec) from the best of 5 executions on a single core of a MacBook Pro with 2.7 GHz intel Core i7 and 16GB of RAM for PyCosmo and CLASS with two different accuracy settings.

k_{\max} (Mpc ⁻¹)	Precision			Speed		
	N_k	PyCosmo $l_{\max} = 50, \epsilon < 3 \times 10^{-5}$	CLASS pk_ref.pre	N_k	PyCosmo $l_{\max} = 30, \epsilon < 3 \times 10^{-4}$	CLASS cl_per mille.pre
0.1	72	1.2	1.1	55	0.28	0.20
1.0	129	2.5	2.8	112	0.68	0.42
10	139	3.1	4.9	122	1.0	0.67
29	144	4.2	9.5	127	1.6	1.3

the precision and speed settings described above. The timings for CLASS are given for a precision setting as described above and a speed setting obtained using the `cl_per mille.pre` precision file. The settings were chosen to achieve an accuracies of about 0.01% and better than 0.1%, respectively, for the transfer function [23], which is comparable to the accuracy of PyCosmo for the corresponding settings. The table also shows results for different maximal wavenumber k_{\max} and number, N_k , of k values evaluated. As the table shows, the timings for PyCosmo and CLASS are comparable for both settings and different k_{\max} .

5. Conclusions

In this paper, we presented PyCosmo, a new cosmological Boltzmann code, and described its special purpose solver based on symbolic manipulations, automatic generation of C++ code and sparsity optimisation. We also showed how the code does not rely on physical approximations for speed-up and uses the consistency among the field equations to adapt the time step. The deviations of the fields from this algebraic relation gives us a self-consistent control of the numerical error. From a performance test, we find that the code achieve comparable execution times for comparable accuracies to current Boltzmann solvers for the computation of the transfer functions in the newtonian gauge. PyCosmo currently does not have all the features of these other solvers, but it is complementary to existing cosmological Boltzmann solvers which rely on more general differential equation solvers and physical approximations, and can be used as an independent test of their numerical solutions. The symbolic representation of the Einstein-Boltzmann equation system in PyCosmo provides a convenient interface to implement extended cosmological models. In future works, we aim to implement more general models beyond flat Λ CDM and with more general gravitational field theories beyond General Relativity. The PyCosmo framework can also be used as a general framework to compute cosmological quantities as well as observables for both interactive and for high-performance batch jobs applications. The computation with PyCosmo of observables such as the CMB angular power spectrum, weak lensing statistics and galaxy clustering statistics is left to a future publication. Information about the PyCosmo package and future code releases are available at <http://www.cosmology.ethz.ch/research/software-lab.html>.

Acknowledgements

The authors thank Andrina Nicola, Aseem Paranjape, Joel Akeret, Oliver Hahn, Sharvari Narkarni-Ghosh and Caroline Bertemes for useful discussions, and Julien Lesgourgues for useful comments and providing CLASS high precision settings for the newtonian gauge. LH thanks financial support from Dr. Max Rösler, the Walter Haefner Foundation and the ETH Zurich Foundation.

References

- [1] C.-P. Ma, E. Bertschinger, Cosmological Perturbation Theory in the Synchronous and Conformal Newtonian Gauges, *ApJ* 455 (1995) 7. [arXiv:astro-ph/9506072](https://arxiv.org/abs/astro-ph/9506072), doi:10.1086/176550.
- [2] E. Bertschinger, COSMICS: Cosmological Initial Conditions and Microwave Anisotropy Codes, *ArXiv Astrophysics e-prints* [arXiv:astro-ph/9506070](https://arxiv.org/abs/astro-ph/9506070).
- [3] U. Seljak, M. Zaldarriaga, A Line-of-Sight Integration Approach to Cosmic Microwave Background Anisotropies, *Astrophysical Journal* 469 (1996) 437. [arXiv:astro-ph/9603033](https://arxiv.org/abs/astro-ph/9603033), doi:10.1086/177793.

- [4] M. Doran, CMBEASY: an object oriented code for the cosmic microwave background, *Journal of Cosmology and Astro-Particle Physics* 10 (2005) 011. [arXiv:astro-ph/0302138](#), doi:10.1088/1475-7516/2005/10/011.
- [5] A. Lewis, A. Challinor, A. Lasenby, Efficient Computation of Cosmic Microwave Background Anisotropies in Closed Friedmann-Robertson-Walker Models, *Astrophysical Journal* 538 (2000) 473–476. [arXiv:astro-ph/9911177](#), doi:10.1086/309179.
- [6] J. Lesgourgues, The Cosmic Linear Anisotropy Solving System (CLASS) I: Overview, *ArXiv e-prints* [arXiv:1104.2932](#).
- [7] A. Lewis, S. Bridle, Cosmological parameters from CMB and other data: A Monte Carlo approach, *Physical Review D* 66 (10) (2002) 103511. [arXiv:astro-ph/0205436](#), doi:10.1103/PhysRevD.66.103511.
- [8] J. Akeret, S. Seehars, A. Amara, A. Refregier, A. Csillaghy, CosmoHammer: Cosmological parameter estimation with the MCMC Hammer, *ArXiv e-prints* [arXiv:1212.1721](#).
- [9] S. Nadkarni-Ghosh, A. Refregier, The Einstein-Boltzmann equations revisited, *ArXiv e-prints* [arXiv:1612.06697](#).
- [10] A. Refregier, A. Amara, T. D. Kitching, A. Rassat, iCosmo: an interactive cosmology package, *Astronomy & Astrophysics* 528 (2011) A33. [arXiv:0810.1285](#), doi:10.1051/0004-6361/200811112.
- [11] S. Dodelson, *Modern cosmology*, 2003.
- [12] S. Seager, D. D. Sasselov, D. Scott, A New Calculation of the Recombination Epoch, *ApJL* 523 (1999) L1–L5. [arXiv:astro-ph/9909275](#), doi:10.1086/312250.
- [13] S. Seager, D. D. Sasselov, D. Scott, How Exactly Did the Universe Become Neutral?, *ApJS* 128 (2000) 407–430. [arXiv:astro-ph/9912182](#), doi:10.1086/313388.
- [14] J. Chluba, R. A. Sunyaev, Cosmological recombination: feedback of helium photons and its effect on the recombination spectrum, *MNRAS* 402 (2010) 1221–1248. [arXiv:0909.2378](#), doi:10.1111/j.1365-2966.2009.15959.x.
- [15] J. Chluba, G. M. Vasil, L. J. Dursi, Recombinations to the Rydberg states of hydrogen and their effect during the cosmological recombination epoch, *MNRAS* 407 (2010) 599–612. [arXiv:1003.4928](#), doi:10.1111/j.1365-2966.2010.16940.x.
- [16] J. A. Rubiño-Martín, J. Chluba, W. A. Fendt, B. D. Wandelt, Estimating the impact of recombination uncertainties on the cosmological parameter constraints from cosmic microwave background experiments, *MNRAS* 403 (2010) 439–452. [arXiv:0910.4383](#), doi:10.1111/j.1365-2966.2009.16136.x.
- [17] J. Chluba, R. M. Thomas, Towards a complete treatment of the cosmological recombination problem, *MNRAS* 412 (2011) 748–764. [arXiv:1010.3631](#), doi:10.1111/j.1365-2966.2010.17940.x.
- [18] J. Chluba, Y. Ali-Haïmoud, COSMOSPEC: fast and detailed computation of the cosmological recombination radiation from hydrogen and helium, *MNRAS* 456 (2016) 3494–3508. [arXiv:1510.03877](#), doi:10.1093/mnras/stv2691.
- [19] E. Bertschinger, COSMICS: Cosmological Initial Conditions and Microwave Anisotropy Codes, *ArXiv Astrophysics e-prints* [arXiv:astro-ph/9506070](#).
- [20] S. Eckert, H. Baaser, D. Gross, O. Scherf, A bdf2 integration method with step size control for elasto-plasticity, *Computational Mechanics* 34 (5) (2004) 377–386. doi:10.1007/s00466-004-0581-1. URL <http://dx.doi.org/10.1007/s00466-004-0581-1>
- [21] V. Menon, K. Pingali, Look left, look right, look left again: An application of fractal symbolic analysis to linear algebra code restructuring, *International Journal of Parallel Programming* 32 (6) (2004) 501–523. doi:10.1023/B:IJPP.0000042084.99636.a0. URL <http://dx.doi.org/10.1023/B:IJPP.0000042084.99636.a0>
- [22] J. Akeret, L. Gamper, A. Amara, A. Refregier, HOPE: A Python just-in-time compiler for astrophysical computations, *Astronomy and Computing* 10 (2015) 1–8. [arXiv:1410.4345](#), doi:10.1016/j.ascom.2014.12.001.
- [23] J. Lesgourgues, The Cosmic Linear Anisotropy Solving System (CLASS) III: Comparision with CAMB for LambdaCDM, *ArXiv e-prints* [arXiv:1104.2934](#).